

ACTIVE MATTER

Low rattling: A predictive principle for self-organization in active collectives

Pavel Chvykov¹, Thomas A. Berrueta², Akash Vardhan³, William Savoie³, Alexander Samland², Todd D. Murphey², Kurt Wiesenfeld³, Daniel I. Goldman³, Jeremy L. England^{3,4,*}

Self-organization is frequently observed in active collectives as varied as ant rafts and molecular motor assemblies. General principles describing self-organization away from equilibrium have been challenging to identify. We offer a unifying framework that models the behavior of complex systems as largely random while capturing their configuration-dependent response to external forcing. This allows derivation of a Boltzmann-like principle for understanding and manipulating driven self-organization. We validate our predictions experimentally, with the use of shape-changing robotic active matter, and outline a methodology for controlling collective behavior. Our findings highlight how emergent order depends sensitively on the matching between external patterns of forcing and internal dynamical response properties, pointing toward future approaches for the design and control of active particle mixtures and metamaterials.

Self-organization in nature is surprising because getting a large group of separate particles to act in an organized way is often difficult. By definition, arrangements of matter we call “orderly” are special, making up a tiny minority of all allowed configurations. For example, we find each unique, symmetrical shape of a snowflake visually striking, unlike any randomly rearranged clump of the same water molecules. Thus, any theory of emergent order in many-particle collectives must explain how a small subset of configurations are spontaneously selected among the vast set of disorganized arrangements.

Spontaneous many-body order is well understood in thermal equilibrium cases such as crystalline solids or DNA origami (1), where the assembling matter is allowed to sit unperturbed for a long time at constant temperature T . The statistical mechanical approach proceeds by approximating the complex deterministic dynamics of the particles with a probabilistic “molecular chaos,” positing that the law of conservation of energy governs otherwise random behavior (2). What follows is the Boltzmann distribution for the steady-state probabilities, $p_{ss}(\mathbf{q}) \propto \exp[-E(\mathbf{q})/T]$, which shows that the degree to which special configurations \mathbf{q} of low energy $E(\mathbf{q})$ have a high probability $p_{ss}(\mathbf{q})$ in the long term depends on the amplitude of the thermal noise. Orderly configurations can assemble and remain stable, so long as interparticle attractions are strong enough to overcome the randomizing effects of thermal fluctuations.

However, there are also many examples of emergent order outside of thermal equilib-

rium. These include “random organization” in sheared colloids (3), phase separation in multitemperature particle mixtures (4), and dynamic vortices in protein filaments (5). A variety of ordered behaviors arise far from equilibrium that cannot be explained in terms of simple interparticle attraction or energy gradients (6–9).

In all of these examples, the energy flux from external sources allows different system configurations to experience fluctuations of different magnitude (10, 11). We suggest that the emergence of such configuration-dependent fluctuations, which cannot happen in equilibrium, may be key to understanding many nonequilibrium self-organization phenomena. In particular, we introduce a measure of driving-induced random fluctuations, which we term rattling $\mathcal{R}(\mathbf{q})$, and argue that it could play a role in many far-from-equilibrium systems similar to the role of energy in equilibrium. We test this in a number of systems, including a flexible active matter system of simple robots we call “smarticles” (smart active particles) (12) as a convenient test platform (see movie S1) inspired by similar robo-physical emulators of collective behavior (13–15). Despite their purely repulsive inter-robot interactions, we find that smarticles spontaneously self-organize into collective “dances,” whose shape and motions are matched to the temporal pattern of external driving forces (movies S2 and S3). This platform and others (16–18), including the nonequilibrium ordering examples mentioned above, all exhibit low-rattling ordered behaviors that echo low-energy structures emergent at equilibrium. We thus motivate and test a predictive theory based on rattling that may explain a broad class of nonequilibrium ordering phenomena.

In devising our approach, we take inspiration from the phenomenon of thermophoresis, which is the simplest example of purely non-

equilibrium self-organization. Thermophoresis is characterized by the diffusion of colloidal particles from hot regions to cold regions (19). If noninteracting particles in a viscous fluid are subject to a temperature $T(\mathbf{q})$ that varies over position \mathbf{q} , their resulting density in the steady-state $p_{ss}(\mathbf{q})$ will concentrate in the regions of low temperature. Particles diffuse to regions where thermal noise is weaker, and they become trapped there. With the diffusivity landscape set by thermal noise locally according to the fluctuation-dissipation relation $D(\mathbf{q}) \propto T(\mathbf{q})$ (20), the steady-state diffusion equation $\nabla^2[D(\mathbf{q})p_{ss}(\mathbf{q})] = 0$ is satisfied by the probability density $p_{ss}(\mathbf{q}) \propto 1/D(\mathbf{q})$. Hence, a low-entropy, “ordered” arrangement of particles can be stable when the diffusivity landscape has a few locations \mathbf{q} that are strongly selected by their extremely low $D(\mathbf{q})$ values.

We seek to extend this intuition to explain nonequilibrium self-organization more broadly. However, a straightforward mathematical extension of the idea encounters challenges in only slightly more complicated scenarios. For an arbitrary diffusion tensor landscape $\mathbf{D}(\mathbf{q})$, in which diffusivity can depend on the direction of motion, one can no longer find general solutions for the steady state. Moreover, the steady-state density $p_{ss}(\mathbf{q})$ at configuration \mathbf{q} may depend on the diffusivity $\mathbf{D}(\tilde{\mathbf{q}})$ at arbitrarily distant configurations $\tilde{\mathbf{q}}$. Nonetheless, we suggest that for most typical diffusion landscapes, the local magnitude of fluctuations $|\mathbf{D}(\mathbf{q})|$ should statistically bias $p_{ss}(\mathbf{q})$ and hence should be approximately predictive of it. This insight, which is central to our theory, is illustrated to hold numerically in Fig. 1A for a randomly constructed two-dimensional anisotropic landscape, and in fig. S3 for higher dimensions. Although contrived counterexamples that break the relationship may be constructed, they require specific fine-tuning (see fig. S4).

The key assumption underlying our approach is that the complex system dynamics are so messy that only the amplitude of local drive-induced fluctuations governs the otherwise random behavior—an assumption inspired by molecular chaos at equilibrium. We expect this to apply when the system dynamics are so complex, nonlinear, and high-dimensional that no global symmetry or constraint can be found for its simplification. Although one cannot predict a configuration’s nonequilibrium steady-state probability from its local properties in the general case (21, 22), the feat becomes achievable in practice for “messy” systems. To illustrate this point explicitly, we consider a discrete dynamical system with random transition rates between a large number of states. Here, we can show analytically that the net rate at which we exit any given state predicts its long-term probability approximately,

¹Physics of Living Systems, Massachusetts Institute of Technology, Cambridge, MA 02139, USA. ²Department of Mechanical Engineering, Northwestern University, Evanston, IL 60208, USA. ³School of Physics, Georgia Institute of Technology, Atlanta, GA 30332, USA. ⁴GlaxoSmithKline AI/ML, 200 Cambridgepark Drive, Cambridge, MA 02140, USA. *Corresponding author. Email: j@englandlab.com

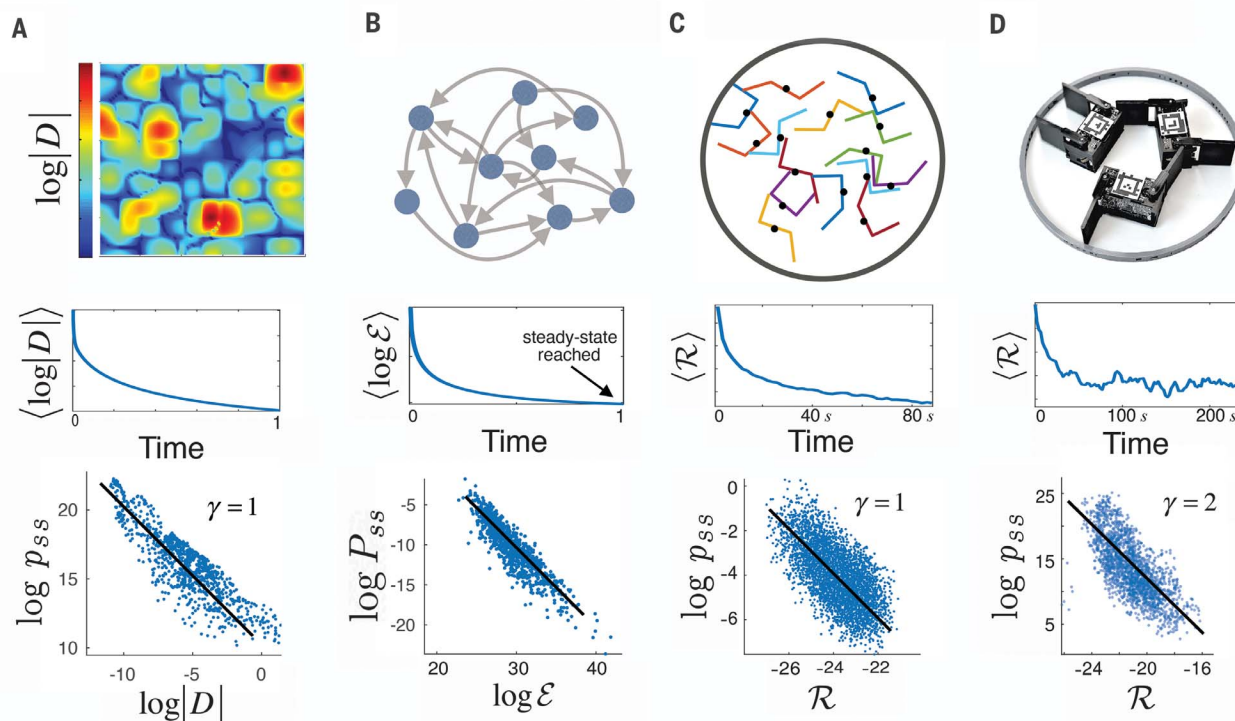


Fig. 1. Rattling \mathcal{R} is predictive of steady-state likelihood across far-from-equilibrium systems. (A) Inhomogeneous anisotropic diffusion in two dimensions, where the steady-state density $p_{ss}(\mathbf{q})$ is seen to be approximately given by the magnitude of local fluctuations $\log|\mathbf{D}(\mathbf{q})| \propto \mathcal{R}(\mathbf{q})$ (where $|\mathbf{D}|$ is the determinant of the diffusion tensor). (B) A random walk on a large random graph (1000 states), where P_{ss} , the probability at a state, is approximately given by \mathcal{E} , that state's exit rate. (C) An active matter system of shape-changing agents: an enclosed ensemble of 15 "smarticles" in simulation. (D) Experimental realization of similar agents with an enclosed three-robot smarticle ensemble. The middle row shows that relaxation to the

steady state of a uniform initial distribution is accompanied by monotonic decay in the average rattling value in all cases, analogous to free energy in equilibrium systems. The bottom row shows the validity of the nonequilibrium Boltzmann-like principle in Eq. 3, where the black lines in (A), (B), and (C) illustrate the theoretical correlation slope for a sufficiently large and complex system (see supplementary materials). The mesoscopic regime in (D) provides the most stringent test of rattling theory (where we observe deviations in γ from 1), while also exhibiting global self-organization. In the middle row, time units are arbitrary in (A) and (B); time is in seconds in (C) and (D), where the drive period is 2 s.

even though the exact result requires global system knowledge (see Fig. 1B and supplementary materials for derivation). This result may be related to the above discussion of thermophoresis by noting that the discrete state exit rates are determined by the continuum diffusivity if our dynamics are built by discretizing the domain of a diffusion process.

To formulate our random dynamics assumption explicitly, we represent the complex system evolution as a trajectory in time $\mathbf{q}(t)$, where the configuration vector \mathbf{q} captures the properties of the entire many-particle system. Our messiness assumption amounts to approximating the full complex dynamics between two points $\mathbf{q}(t)$ and $\mathbf{q}(t + \delta t)$ by a random diffusion process. To this end, we take the amplitude of the noise fluctuations $D(\mathbf{q})$ to locally reflect the amplitude of the true configuration dynamics: $|\mathbf{q}(t + \delta t) - \mathbf{q}(t)|^2 \propto D(\mathbf{q})\delta t$ for short rollouts $\mathbf{q}(t \rightarrow t + \delta t)$ (i.e., samples of system trajectories) of duration δt initialized in configuration $\mathbf{q}(t) = \mathbf{q}$ (see supplementary materials for details). Through this approximation, our dynamics are effectively reduced to diffu-

sion in \mathbf{q} -space, which then allows us to locally estimate the steady-state probability of system configurations from $D(\mathbf{q})$ as in thermophoresis. Hence, the global steady-state distribution may be predicted from the properties of short-time, local system rollouts.

For rare orderly configurations to be strongly selected in a messy dynamical system, the landscape of local fluctuations must vary in magnitude over a large range of values. Whereas in thermophoresis these fluctuations are directly imposed by an external temperature profile, in driven dynamical systems the range of magnitudes results from the way a given pattern of driving can have a different effect on different system configurations. The $D(\mathbf{q})$ landscape is emergent from the interplay between the pattern of driving and the library of possible \mathbf{q} -dependent system response properties. In practice, we observe that the amplitudes of system responses to driving do often vary over several orders of magnitude (Fig. 1). We see this phenomenology in many well-known examples of active matter self-organization (3, 11, 23). For example, the crystals that form

in suspensions of self-propelled colloids in (24) may be seen as the collective configurations that respond least diffusively to driving by precisely balancing the propulsive forces among individual particles. This illustrates how the low- $D(\mathbf{q})$ configurations are selected in the steady state by an exceptional matching of their response properties to the way the system is driven.

We apply these ideas in real complex driven systems whose response to driving we cannot predict analytically, such as our robotic swarm of smarticles. In this case, we require an estimator for the local value of $D(\mathbf{q})$ based on observations of short rollouts of system behavior. The estimator of the local diffusion tensor that we choose here is the covariance matrix

$$\mathcal{C}(\mathbf{q}) = \text{cov}[\tilde{\mathbf{v}}_{\mathbf{q}}, \tilde{\mathbf{v}}_{\mathbf{q}}] \quad (1)$$

(25), where $\tilde{\mathbf{v}}_{\mathbf{q}}$ is seen as a random variable with samples drawn from $\{(\tilde{\mathbf{q}}(t) - \tilde{\mathbf{q}}(0))/\sqrt{t}\}_{\mathbf{q}(0)=\mathbf{q}}$ at various time points t along one or several short system trajectories $\tilde{\mathbf{q}}(t)$ rolled

out from $\tilde{\mathbf{q}}(0) = \mathbf{q}$. We assume these rollouts $\tilde{\mathbf{q}}(t)$ to be long enough to capture fluctuations in the configuration variables under the influence of a drive, but short enough to have $\tilde{\mathbf{q}}(t)$ stay near \mathbf{q} (see supplementary materials for details).

Although the covariance matrix reflects the amplitude of local fluctuations, we are instead interested in a measure of their disorder if we want to estimate the effective diffusivity. This follows from the observation that high-amplitude ordered oscillations do not contribute to the rate of stochastic diffusion (10). We suggest that the degree of disorder of fluctuations may be captured by the entropy of the distribution of $\tilde{\mathbf{v}}_{\mathbf{q}}$ vectors, which is how we define rattling $\mathcal{R}(\mathbf{q})$. Physically, vectors $\tilde{\mathbf{v}}_{\mathbf{q}}$ capture the statistics of the force fluctuations experienced in configuration \mathbf{q} , and so rattling measures the disorder in the system's driven response properties at that point. By approximating the distribution of $\tilde{\mathbf{v}}_{\mathbf{q}}$ as Gaussian, we can express its entropy (up to a constant offset) simply in terms of $\mathcal{C}(\mathbf{q})$ as

$$\mathcal{R}(\mathbf{q}) = \frac{1}{2} \log \det \mathcal{C}(\mathbf{q}) \quad (2)$$

With this definition, we generalize the thermophoretic expression for the steady-state density

$p_{ss}(\mathbf{q}) \propto 1/D(\mathbf{q})$ and express it in a Boltzmann-like form:

$$p_{ss}(\mathbf{q}) \propto \exp[-\gamma \mathcal{R}(\mathbf{q})] \quad (3)$$

where γ is a system-specific constant of order 1 (see supplementary materials for derivations). We note that when energy varies on the same scale as rattling, the interaction between the two landscapes can generate strong steady-state currents and may break this relation (10). Thus, rattling enables us to predict the long-term global steady-state distribution based on empirical measurements of short-term local system behavior, which suggests that probability density accumulates over time in low-rattling configurations.

We study the collective behavior of a simple ensemble of smarticles, aligning ourselves within the tradition of using robotic systems as flexible, physical emulators for self-organizing natural systems (13–16). Each smarticle (Fig. 2A) is composed of three 5.2-cm links, with two hinges actuated by motors programmed to follow a driving pattern specified by a microcontroller. When a smarticle sits on a flat surface, its arms do not touch the ground, so an individual robot cannot move. However, a group of them can achieve complex motion by pushing and pulling each other (movie S1) (26). The relative coordinates of the middle

link of each robot in the ensemble (x, y, θ) may be thought of as the internal system configurations that dynamically respond to an externally determined driving force arising from the time variation of arm angles (α_1, α_2) (27).

This robotic active matter system offers substantial flexibility in choosing the programmed patterns of driving as well as the properties of internal system dynamics (friction coefficients, weights, etc.). Additionally, the smarticle system has a flat potential energy landscape, allowing one to focus on the contributions of the drive-induced fluctuations to the collective behavior, which makes our findings broadly applicable to other strongly driven systems. When the smarticles are within contact range (as ensured by a confining ring; Fig. 1D), the forces experienced throughout the collective for a given pattern of arm movement are an emergent function of all system coordinates. This configuration-dependent forcing gives rise to varying rattling values, which we refer to as the “rattling landscape,” and which we see to be a hallmark property in many far-from-equilibrium examples. The rattling landscape then leads to some system configurations being dynamically selected over others and allowing for self-organization, just as the diffusivity landscape does in thermophoresis. Finally, the combined effects of impulsive inter-robot

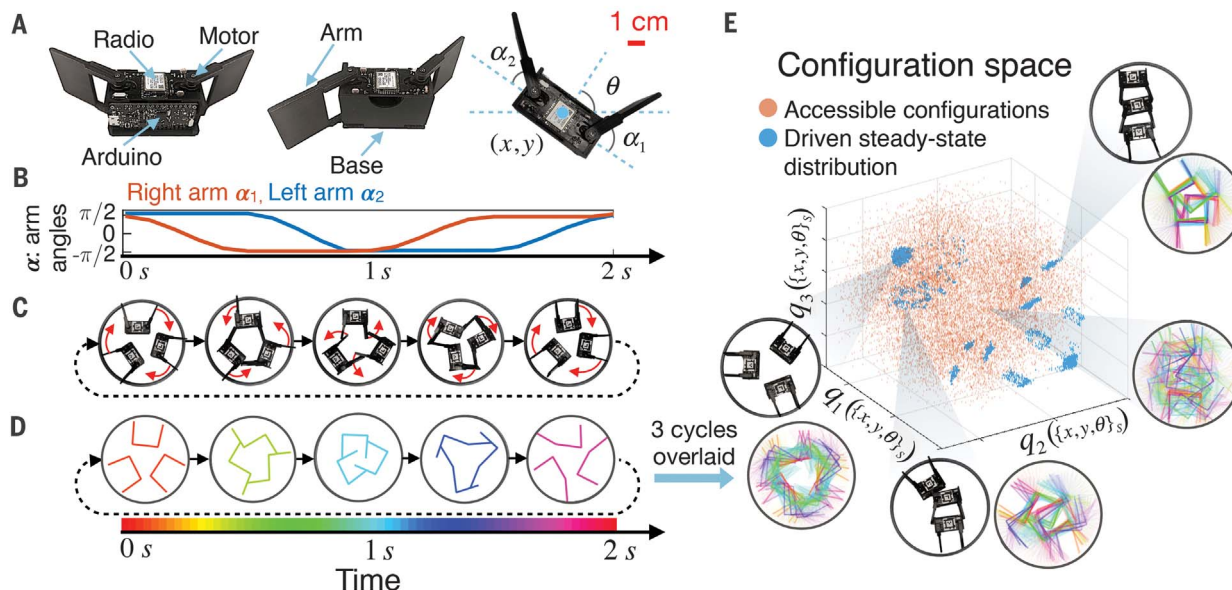


Fig. 2. Self-organization in a smarticle robotic ensemble. (A) Front, back, and top views of a single smarticle. Of its five degrees of freedom, we consider the time-varying arm angles (α_1, α_2) as “external” driving, because these are controlled by a preprogrammed microcontroller, whereas the robot coordinates (x, y, θ) are seen as an “internal” system configuration, because these respond interdependently to the arms. (B) An example of a periodic arm motion pattern. (C) Top view of three smarticles confined in a fixed ring, all programmed to synchronously execute the driving pattern shown in (B). The video frames, aligned on the time axis of (B), show one example of dynamically ordered collective “dance” that can spontaneously

emerge under this drive [see (E) and movie S3 for others]. (D) Simulation video showing agreement with experiment in (C). We color-code simulated states periodically in time and overlay them for three periods to illustrate the dynamical order over time. (E) The system’s configuration space, built from nonlinear functions of the three robots’ body coordinates (x, y, θ). The steady-state distribution (blue) illustrates the few ordered configurations that are spontaneously selected by the driving out of all accessible system states (orange). Simulation data are shown; see fig. S5B for experimental data and fig. S1 for details of how the configuration space coordinates (q_1, q_2, q_3) in (E) are constructed from the $3 \times (x, y, \theta)$ coordinates.

collisions, nonlinear boundary interactions, and static friction lead to a large degree of quasi-random motion (26), making this a promising candidate system for exploring our theory.

Reasoning that our fundamental assumption of quasi-random configuration dynamics would be most valid in systems with many degrees of freedom, we also built a simulation that would allow us to study the properties of larger smarticle groups and explore different system parameters (fig. S9). In this regime, we used simulations to gather enough data to sample the high-dimensional probability distributions for our analysis. In a simulation of 15 smarticles, we observed the tendency of the ensemble to reduce average rattling over time after a random initialization. For this 45-dimensional system (x, y, θ for 15 robots), the configuration-space dynamics are well approximated by diffusion, and so Eq. 3 holds, as seen in Fig. 1C. In addition, we noted the emergence of metastable pockets of local order when groups of three or four nearby smarticles self-organized into regular motion patterns for several drive cycles (movie S2). A signature of such dynamical heterogeneity can be seen in the spectrum of the covariance matrix $C(\mathbf{q})$ from Eq. 1, as described in the supplementary materials and fig. S10.

The transient appearance of dynamical order in subsets of smarticle collectives raises the question of whether our rattling theory continues to hold for smaller ensembles. For the remainder of this paper, we focus on ensembles of three smarticles (as in Fig. 1D), which allows for exhaustive sampling of configurations experimentally, as well as easier

visualization of the configuration space (as in Fig. 2E). Both in simulation and experiment, we found that this regime exhibits a variety of low-rattling behaviors that manifest as distinct, orderly collective “dances” (Fig. 2, C and D, and movie S3). Despite its small size, this system is well described by rattling theory, as evidenced by the empirical correlation between rattling and the steady-state likelihood of configurations (Fig. 1D, bottom).

We consider self-organization as a consequence of a system’s landscape of rattling values over configuration space. This rattling landscape is specific to the particular drive forcing the system out of equilibrium, because different drives will generally produce different dynamical responses in the same system configuration. When the three-smarticle ensemble is driven (under the pattern in Fig. 2B), the range of observed rattling values is so large that the lowest-rattling configurations—and consequently those with the highest likelihood—account for most of the steady-state probability mass. More than 99% of probability accumulates in these spontaneously selected configurations, which represent only 0.1% of all accessible system states (Fig. 2E). Moreover, in these configurations the smarticles exhibit an orderly response to driving (Fig. 2, C and D, and movie S4). In practice, the ensemble spends most of its time in or nearly in one of several distinct dances, with occasional interruptions by stochastic flights from one such dynamical attractor to another (movie S5).

From the above observations, we can begin to understand self-organization in driven collectives. In equilibrium, order arises when its entropic cost is outweighed by the available

reduction of energy. Analogously, a sufficiently large reduction in rattling can lead to dynamical organization in a driven system. Moreover, such a reduction can require matching between the system dynamics and the drive pattern.

Through rattling theory we can predict how self-organized states are affected by changes in the features of the drive. We expect the structure of the self-organized dynamical attractors to be specific to the driving pattern, as each drive induces its own rattling landscape. To test this, we programmed the three smarticles with two distinct driving patterns (Fig. 3, A and B, top), which we ran separately. The two resulting steady-state distributions, although each is highly localized to a few configurations, are largely non-overlapping (Fig. 3, A and B, bottom). This indicates that by tuning the drive pattern, it may be possible to design the structure of the resulting steady state, and hence to control the self-organized dynamics [see also (28–30)].

As a proof of principle for such control, we developed a methodology for selecting particular steady-state behaviors by combining drives. By randomly switching back and forth between drives A and B in Fig. 3, we define a compound drive A+B (Fig. 3C and movie S6). We predicted that this drive would select only those configurations common to both A and B steady states (Fig. 3, A and B, bottom), because having low rattling under this mixed drive requires having low rattling under both constituent drives. Our experiments confirmed this (Fig. 3C), and we were further able to quantitatively predict the probability that a configuration would appear under the mixed drive on the basis of its

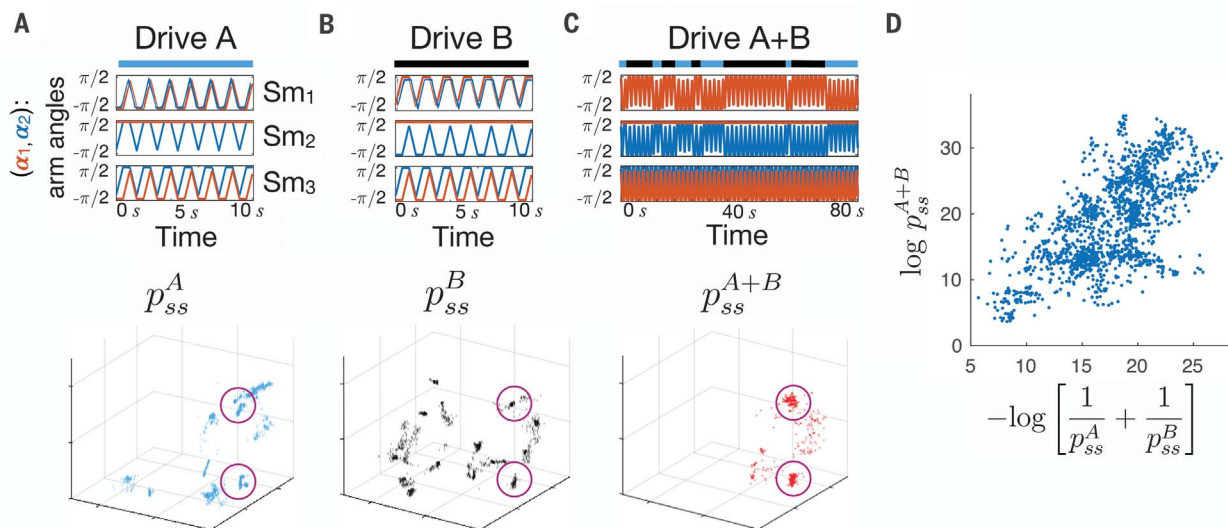


Fig. 3. Self-organized behaviors are fine-tuned to drive pattern. (A and B) Changing the arm motion pattern slightly (top) affects which configurations self-organize in the steady state (bottom, same 3D configuration space as in Fig. 2E). (C) By mixing drives A and B as shown (top), we can isolate only those

configurations selected in both the steady states (circled in purple; see movie S6), which follows as an analytical prediction of the theory. (D) This prediction (Eq. 4) is quantitatively verified. All data shown are experimental and are reproduced in simulation in fig. S7, along with derivations in the supplementary materials.

likelihood in each constituent steady state according to

$$\frac{1}{p_{ss}^{A+B}} \propto \frac{1}{p_{ss}^A} + \frac{1}{p_{ss}^B} \quad (4)$$

as shown in Fig. 3D and fig. S7 (see supplementary materials for derivation). This simple relationship suggests that by composing

different drives in time, one can single out desired configurations for the system steady state.

Moreover, we show that we can analytically predict and control the degree of order in the system by tuning drive randomness (Fig. 4) as well as internal system friction (movie S7, fig. S8, and supplementary materials). Because driven self-organization arises when the sys-

tem has access to a broad range of rattling values, tuning it requires modulating the rattling of the most ordered behaviors relative to the background high-rattling states.

We can directly manipulate the rattling landscape by modulating the entropy of the drive pattern. This is done by introducing a probabilistic element to the programmed arm motion. At each move, we introduce a probability of making a random arm movement not included in the prescribed drive pattern. Increasing this probability results in flattening the rattling landscape: Ordered states experience an increase in rattling due to drive entropy, whereas states whose rattling is already high do not (Fig. 4A). Correspondingly, the steady-state distributions become progressively more diffuse (Fig. 4B), causing localized pockets of order to give way to entropy and “melt” away—just as crystals might in equilibrium physics [movie S8; see also (37)].

Even as the range of accessible rattling values in the system shrinks, the predictive relation of Eq. 3 continues to hold (Fig. 4C), enabling quantitative prediction of how self-organized configurations are destabilized. By calculating the entropy of the drive pattern as we tune its randomness, we derive a lower bound on rattling for the system. Thus, we can analytically predict how steady-state probabilities change as a function of drive randomness, as shown in Fig. 4D (up to normalization and γ ; see supplementary materials for derivation). This result confirms the simple intuition that more predictably patterned driving forces offer greater opportunity for the system to find low-rattling configurations and self-organize (see also fig. S6).

Our findings suggest that the complex dynamics of a driven collective of nonlinearly interacting particles may give rise to a situation in which a new kind of simplicity emerges. We have shown that when quasi-random transitions among configurations dominate the dynamics, the steady-state likelihood can be predicted from the entropy of local force fluctuations, which we refer to as rattling. In what we term a “low-rattling selection principle,” configurations are selected in the steady state according to their rattling values under a given drive.

Low rattling provides the basis for self-organized dynamical order that is specifically selected by the choice of driving pattern. We see analytically and experimentally that the degree of order in the steady-state distribution reflects the predictability of patterns in driving forces. Thus, driving patterns with low entropy pick out fine-tuned configurations and dynamical trajectories to stabilize. This makes it possible for one collective to exhibit different modes of ordered motion depending on the fingerprint of the external driving. These modes differ in their emergent collective properties,

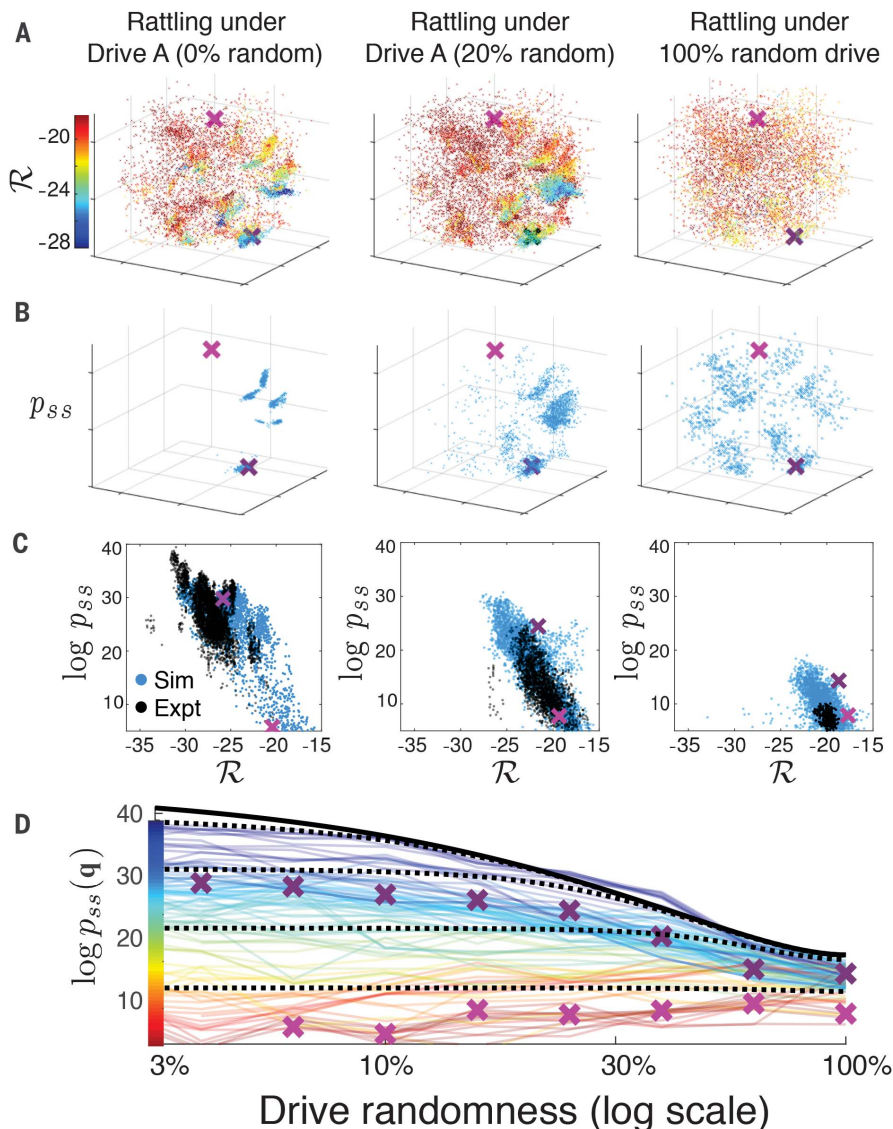


Fig. 4. Tuning self-organization by modulating drive randomness. Self-organization relies on the degree of predictability in its driving forces, in a way that we can quantify and compute analytically. **(A)** As the drive becomes less predictable (left to right in all panels), low-rattling configurations gradually disappear. **(B)** The corresponding steady states, reflecting the low-rattling regions of **(A)**, become accordingly more diffuse. [**(A)** and **(B)** show simulation data and use the same 3D configuration space as Fig. 2E]. **(C)** All three correlations fall along the same line (blue, simulation; black, experiment), verifying that our central predictive relation (Eq. 3) holds for all drives here. The diminishing range of rattling values thus precludes strong aggregation of probability, and with it self-organization. **(D)** Our theoretical prediction (solid black line) indicating how the most likely configurations are destabilized by drive randomness. Colored lines track the probability p_{ss} at 100 representative configurations \mathbf{q} in simulation, and dashed black lines analytically predict their trends. (movie S8; see supplementary materials for derivation). Two specific configurations marked by pink and purple crosses are tracked across analyses.

which suggests “top-down” alternatives to control of active matter and metamaterial design, where ensemble behaviors, rather than being microscopically engineered, are dynamically self-selected by the choice of driving (30, 32).

REFERENCES AND NOTES

1. P. W. K. Rothmund, *Nature* **440**, 297–302 (2006).
2. M. Kardar, *Statistical Physics of Particles* (Cambridge Univ. Press, 2007).
3. L. Corté, P. Chaikin, J. P. Gollub, D. Pine, *Nat. Phys.* **4**, 420–424 (2008).
4. A. Y. Grosberg, J.-F. Joanny, *Phys. Rev. E* **92**, 032118 (2015).
5. Y. Sumino *et al.*, *Nature* **483**, 448–452 (2012).
6. S. Ramaswamy, *Annu. Rev. Condens. Matter Phys.* **1**, 323–345 (2010).
7. L. Bertini, A. De Sole, D. Gabrielli, G. Jona-Lasinio, C. Landim, *Rev. Mod. Phys.* **87**, 593–636 (2015).
8. M. Paoluzzi, C. Maggi, U. Marini Bettolo Marconi, N. Gnan, *Phys. Rev. E* **94**, 052602 (2016).
9. T. Speck, *Europhys. Lett.* **114**, 30006 (2016).
10. P. Chvykov, J. England, *Phys. Rev. E* **97**, 032115 (2018).
11. M. E. Cates, J. Tailleur, *Annu. Rev. Condens. Matter Phys.* **6**, 219–244 (2015).
12. W. Savoie, thesis, Georgia Institute of Technology (2019).
13. J. Aguilar *et al.*, *Science* **361**, 672–677 (2018).
14. M. Rubenstein, A. Cornejo, R. Nagpal, *Science* **345**, 795–799 (2014).
15. J. Werfel, K. Petersen, R. Nagpal, *Science* **343**, 754–758 (2014).
16. S. Li *et al.*, *Nature* **567**, 361–365 (2019).
17. G. Vásárhelyi *et al.*, *Sci. Robot.* **3**, eaat3536 (2018).
18. S. Mayya, G. Notomista, D. Shell, S. Hutchinson, M. Egerstedt, in *IEEE/RSJ International Conference on Intelligent Robots and Systems (IROS)*, Macau, China (2019), pp. 4106–4112.
19. S. Dühr, D. Braun, *Proc. Natl. Acad. Sci. U.S.A.* **103**, 19678–19682 (2006).
20. N. G. Van Kampen, *Stochastic Processes in Physics and Chemistry, vol. I* (Elsevier, 1992).
21. R. Landauer, *Physica A* **194**, 551–562 (1993).
22. R. Landauer, *Phys. Rev. A* **12**, 636–638 (1975).
23. G. S. Redner, M. F. Hagan, A. Baskaran, *Phys. Rev. Lett.* **110**, 055701 (2013).
24. J. Palacci, S. Sacanna, A. P. Steinberg, D. J. Pine, P. M. Chaikin, *Science* **339**, 936–940 (2013).
25. X. Michalet, A. J. Berglund, *Phys. Rev. E* **85**, 061916 (2012).
26. W. Savoie *et al.*, *Sci. Robot.* **4**, eaax4316 (2019).
27. See supplementary materials.
28. H. Kedia, D. Pan, J.-J. Slotine, J. L. England, arXiv 1908.09332 [nlin.AO] (25 August 2019).
29. T. Epstein, J. Fineberg, *Phys. Rev. Lett.* **92**, 244502 (2004).
30. H. Karani, G. E. Pradillo, P. M. Vlahovska, *Phys. Rev. Lett.* **123**, 208002 (2019).
31. D. I. Goldman, M. D. Shattuck, S. J. Moon, J. B. Swift, H. L. Swinney, *Phys. Rev. Lett.* **90**, 104302 (2003).
32. O. Sigmund, in *IUTAM Symposium on Modelling Nanomaterials and Nanosystems* (Springer, 2009), pp. 151–159.
33. T. A. Berrueta, A. Samland, P. Chvykov, Repository with all data, hardware, firmware, and software files needed to recreate the results of this manuscript: <https://doi.org/10.5281/zenodo.4056700>.

ACKNOWLEDGMENTS

We thank P. Umbanhowar, H. Kedia, and J. Owen for helpful discussions. **Funding:** Supported by ARO grant W911NF-18-1-0101 and James S. McDonnell Foundation Scholar grant 220020476 (P.C. and J.L.E.); ARO MURI award W911NF-19-1-0233 and NSF grant CBET-1637764 (T.A.B., A.S., and T.D.M.); NSF grants PoLS-0957659, PHY-1205878, and DMR-1551095 and ARO grant W911NF-13-1-0347 (A.V., W.S., and D.I.G.); and NSF grant PHY-1205878 (K.W.). **Author contributions:** P.C. derived all theoretical results, performed simulations, data analysis, and contributed to writing; T.A.B. performed all experiments in the main text and contributed to writing and data analysis; A.V. and W.S. performed supplementary experiments; A.S. aided in robot hardware and software fabrication; and J.L.E., D.I.G., K.W., and T.D.M. secured funding and provided guidance throughout. **Competing interests:** The authors declare no competing interests. **Data and materials availability:** All files needed for fabricating smarticles, as well as representative data, can be found in (33).

SUPPLEMENTARY MATERIALS

science.sciencemag.org/content/371/6524/90/suppl/DC1
Materials and Methods
Supplementary Text
Figs. S1 to S10
References (34–46)
Movies S1 to S8

6 May 2020; accepted 27 November 2020
10.1126/science.abc6182